

The 2001 Bhuj earthquake: Tomographic evidence for fluids at the hypocenter and its implications for rupture nucleation

J. R. Kayal

Geological Survey of India, Calcutta, India

Dapeng Zhao and O. P. Mishra

Geodynamics Research Center, Ehime University, Matsuyama, Japan

Reena De and O. P. Singh

Geological Survey of India, Calcutta, India

Received 20 March 2002; revised 23 May 2002; accepted 3 June 2002; published 18 December 2002.

[1] The January 26, 2001 Bhuj earthquake (Mw 7.6) is one of the most catastrophic Indian earthquakes. We have investigated the 3-D seismic velocity and Poisson's ratio structures of the Bhuj source area to understand the probable cause of triggering the earthquake. We used 1948 P and 1865 S-wave high-quality arrival times from 331 aftershocks recorded at a temporary seismic network. Significant variations up to 5% in velocity and 10% in Poisson's ratio are revealed in the aftershock area. The mainshock is located in a distinctive zone characterized by high- V_p , low- V_s and high Poisson's ratio (σ) in the depth range of 20 to 30 km and extending 15 to 30 km laterally. This feature is very similar to that of the 1995 Kobe earthquake [Zhao *et al.*, 1996]. The anomaly may be due to a fluid-filled, fractured rock matrix, which might have contributed to the initiation of the Bhuj earthquake. **INDEX TERMS:** 7209 Seismology: Earthquake dynamics and mechanics; 7205 Seismology: Continental crust (1242); 7223 Seismology: Seismic hazard assessment and prediction; 7230 Seismology: Seismicity and seismotectonics; 6982 Adio Science: Tomography and imaging; **KEYWORDS:** Tomographic evidence, Velocity structure, Poisson's ratio. **Citation:** Kayal, J. R., D. Zhao, O. P. Mishra, R. De, and O. P. Singh, The 2001 Bhuj earthquake: Tomographic evidence for fluids at the hypocenter and its implications for rupture nucleation, *Geophys. Res. Lett.*, 29(24), 2152, doi:10.1029/2002GL015177, 2002.

1. Introduction

[2] The devastating Bhuj earthquake of January 26, 2001, magnitude Mw 7.6, occurred in the Kutch rift basin in the Gujrat province of western margin of Peninsular India (Figure 1), which resulted in severe casualties (about 20,000) [Ravi Shanker and Pande, 2001]. The Kutch area falls in the highest seismic zone in the recent seismic zoning map of India [Krishna, 1992]. The Kutch, Cambay and Narmada rifts are the three major rift-basins in the western margin of Peninsular India craton (Figure 1a). These rift-basins are bounded by three important Precambrian tectonic trends: the NNW-SSE Dharwar trend, the NE-SW Delhi-Aravalli trend and the ENE-WSW Satpura trend, which dominate the structural fabric of western India [Biswas,

1987]. All the three basins originated in different periods during the Mesozoic. Among the major earthquakes in Peninsular India, the largest intraplate event was the June 1819 Kutch earthquake (M_L 8.4, Mw 7.8) [Johnston and Kanter, 1990], which had intensity XI on MM scale [Oldham, 1926]. A remarkable feature of this earthquake was the creation of an 80 to 90 km long elevated tract of land, known as "Allah Bund" (Dam of God), close to the India and Pakistan border (Figure 1). The July 21, 1956 Anjar earthquake (Ms 6.1) occurred very close to the January 26, 2001 Bhuj earthquake (Figure 1). The other significant earthquakes near to the study region are shown in Figure 1, which have reverse faulting mechanisms [Kayal *et al.*, 2002].

[3] The Geological Survey of India established a 12-station temporary seismograph network (consisting of 8 analog and 5 digital instruments) in the mainshock epicenter area to monitor the aftershocks from January 29 to April 15, 2001 [Kayal *et al.*, 2002]. One station at Rapar (RPR) was installed with analog and digital instruments simultaneously for comparison. The network design and the major geological features are shown in Figure 1b. Details of the aftershock investigation are given by Kayal *et al.* [2002].

2. Data and Method

[4] In this study we have used the arrival time data of 331 events, which are selected from more than 3000 aftershocks ($M > 1.0$) to determine the 3-D crustal structure of the source area for understanding the rupture nucleation process of the Bhuj earthquake. The epicentral distribution of these events has been shown in both plane and 3-D in Figures 2a and 2b, respectively. All the 331 events were recorded at least by 4 stations and have more than 4 P- and 3 S-arrivals. A total of 3813 arrival time data (1948 P and 1865 S arrivals) from the 331 events are used in this analysis. The reading accuracy is varying from 0.01–0.1 s for P and 0.05–0.3 s for S arrivals.

[5] We have used the tomographic method of Zhao *et al.* [1992] to analyze the selected arrival times and to determine the 3-D P- and S-wave velocity (V_p , V_s) and Poisson's ratio (σ) structures in the source area. We used the 1-D velocity model of Kayal *et al.* [2002] as our starting model. This model incorporates a P- wave velocity of 4.3 km/s for the upper 3 km thick Mesozoic sediments, 5.7 km/s at depth 3–

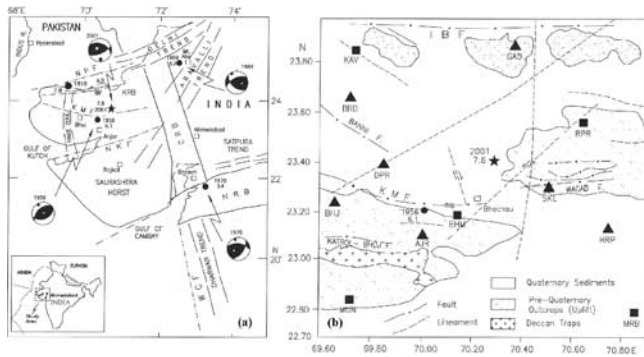


Figure 1. (a) Map showing tectonic features of the study region [compiled from *Biswas, 1987; GSI, 2000, and Talwani and Gangopadhyay, 2001*]. KRB: Kutch Rift Basin; CRB: Cambay Rift Basin; NRB: Narmada Rift Basin; NPF: Nagar Parkar Fault; IBF: Island Belt Fault; KMF: Kutch Mainland Fault; NKF: North Kathiwar Fault; WCF: West Coast Fault; AB: “Allah Bund” (see text). Epicenters (solid circles) and fault-plane solutions of the past significant earthquakes ($M > 5.0$) are shown. For fault-plane solutions, the solid circle indicates P-axis in the dilatational zone, and the open circle T-axis in the compressional zone. The star indicates the mainshock epicentre of the January 26, 2001 Bhuj earthquake. The inset map shows the major plate boundaries around India and the present study area. (b) Map showing the GSI temporary seismic network and the surface geology in the Bhuj area [*GSI, 2000*]. The triangles (analog seismic stations); The solid rectangles (digital seismic stations); The star (Bhuj mainshock).

6 km, 6.2 km/s at depth 6–20.5 km, 7.0 km/s between 20.5 and 37 km, and a mantle velocity 8.1 km/s beneath 37 km and corresponding S- wave velocity for said layers are incorporated in the model from the relation $V_p/V_s = 1.732$.

3. Results and Discussion

[6] We simultaneously inverted for the velocity structure and hypocentral locations of the 331 aftershocks using the tomographic method. The accuracy of hypocenter locations is better than 4 km. The distribution of the relocated aftershocks is shown in Figure 2a. The 3-D plot (Figure 2b) of the hypocenters shows that most of the aftershocks occurred at a depth range varying from 15 to 37 km, while there are few events in the upper crust (depth 0–15 km), which may indicate the presence of an aseismic layer at 10–15 km depth [*Kayal et al., 2002*].

[7] The V_p , V_s , and σ structures are imaged at 5 km depth intervals (5 km–35 km), and some representative results are shown in Figure 3. The images obtained at different depths clearly demonstrate that strong lateral heterogeneities are present in the aftershocks areas of the Bhuj earthquake. The tomographic images for V_p , V_s , and σ show a consistent result at depths of 10–15 km (Figures 3a–3f). The V_p and V_s images show an alternate low and high velocity zones (LVZ and HVZ) while the σ imaging depicts a low poisson’s ratio (low- σ) structure at the abovementioned depths. It may be noticed that aftershocks are much less at shallower depths

(0–10 km) and they are mostly diffused in the LVZ around the main shock epicenter area.

[8] The images of V_p , V_s and σ at depths of 20 km and 25 km reveal very interesting structures (Figures 3g–3l). It is also intriguing to note that the mainshock hypocenter is associated with high- V_p , high- σ to the west and low- V_p , low- σ to its east at 20 km depth (Figures 3g and 3i). This indicates that the fault zone of the mainshock hypocenter is associated with a considerable amount of velocity asperities, and the degree of the coupling on either side of mainshock is different due to different seismic strengths of the fault on both sides of the mainshock. The Figures 3j–3l depict the tomographic images at the depth of 25 km, which is the source area of the Bhuj mainshock. It is interesting to note that the low- V_p , low- σ are no longer visible at this depth level in the V_p and σ images, respectively, while the mainshock hypocenter zone falls in the low- V_s zone. Thus the Bhuj mainshock has occurred in a distinct zone, which is characterized by high- V_p , low- V_s and high- σ , where most of the aftershocks are also located.

[9] The cross-sectional images (Figures 4a–4f) conspicuously indicate that the features are more or less consistent

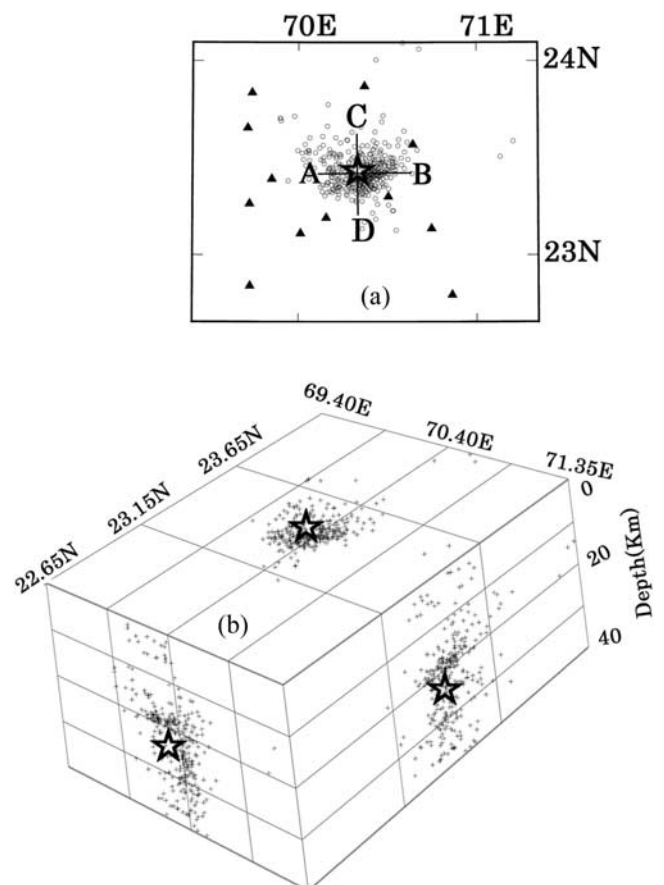


Figure 2. (a) Epicentral distribution in plane of the 331 earthquakes used in this study. The open circles (aftershocks); The star (Bhuj mainshock). Lines A–B and C–D show the locations of the cross sections in Figures 4a–4c and Figures 4d–4f, respectively; The solid triangles (portable seismic stations). (b) 3-D distribution of hypocenters of 331 earthquakes used in this study. Crosses denote aftershocks.

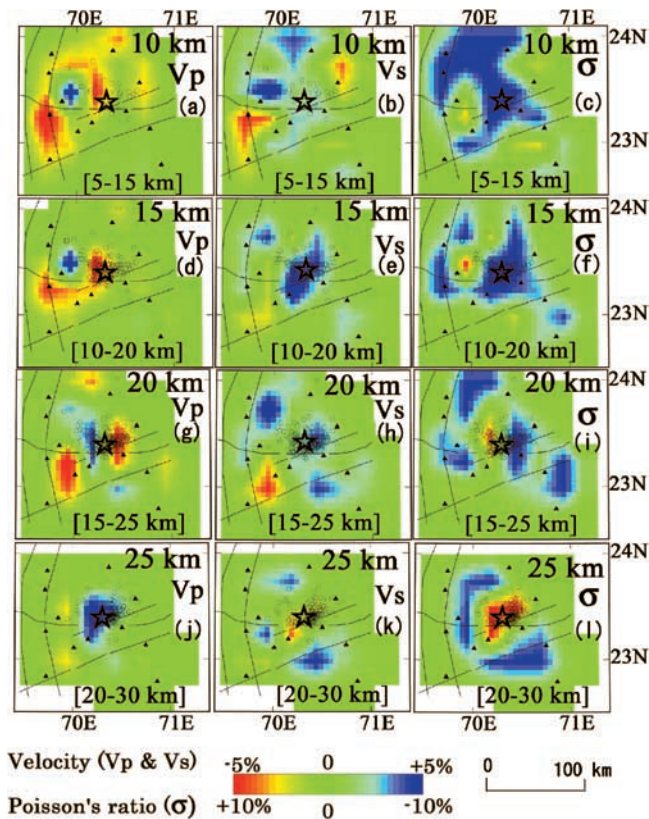


Figure 3. Distribution of V_p , V_s , and σ perturbations (in %) from average velocity at different depths. The depth range of aftershocks (open circle) are shown at the bottom of the respective map. The depth of each layer is shown at the upper-right corner of each map. The dark lines, active faults and lineaments; The solid triangles, portable seismic stations; The star, Bhuj mainshock. The perturbation scale is shown at the bottom.

at shallower depths (5 and 10 km), but they differ in the mid-crust and in the lower crustal depths (15, 20 and 25 km). The V_s is higher in the aftershock source area at 15 and 20 km depths. The anomalies (V_p , V_s and σ) near mainshock hypocenter area at a depth of 25 km (Figures 4a–4f) extend laterally about 15 to 30 km and to depths of about 20 to 30 km. A similar observation was reported for the 1995 Kobe earthquake [Zhao *et al.*, 1996; Zhao and Negishi, 1998]. The 1993 Killari (Central India) earthquake (mb 6.3) source area has also depicted a similar trend for P-wave and S-wave velocities [Kayal and Mukhopadhyay, 2002]. The deeper seismic images at depths of 30 and 35 km (Figures 4a–4f) do not show a LVZ. The aftershocks in this depth range are in the vicinity of the HVZ and high- σ . We, therefore, suggest that this might have acted as a zone for stress accumulation, which may represent the base of the palio-rift [Kayal *et al.*, 2002].

[10] High- V_p anomalies in some parts of the source zones demonstrate that the earthquakes occurred in the most competent part of the rocks, which may be rigid and capable to store strain energy and release it as a brittle failure. Such results have also been reported previously elsewhere in the world [Lees, 1990; Zhao and Kanamori, 1993, 1995; Srinagesh *et al.*, 2000]. But our present result is compar-

tively comprehensive in sense that the source zone of Bhuj earthquake is characterized not only by high- V_p but also by low- V_s and high- σ , which shed a light on the hidden fact that the source zone is decoupled due to the presence of fluid rock matrix. The V_s image is different from that of V_p , probably because S waves are more sensitive to the fluid content of the rock than are P waves [O'Connell and Budiansky, 1974; Zhao *et al.*, 1996]. Our present results are also in good agreement with the earlier results obtained by Zhao *et al.* [1996] for the 1995 Kobe earthquake.

[11] Many researchers have shown that some earthquake nucleation zones exhibit low-velocity, high V_p/V_s ratio and/or high electrical conductivity and subsequently proposed that overpressurized fluids exist in the fault zone [Eberhart-Phillips and Michael, 1993; Gupta *et al.*, 1996; Thurber *et al.*, 1997; Zhao *et al.*, 1996]. Potential sources of fluids may be due to dehydration of minerals, fluids trapped in the pore-spaces, and meteoric water [Zhao *et al.*, 1996; Zhao and Negishi, 1998].

[12] We have performed rigorous checkerboard resolution tests [Zhao *et al.*, 1992] for both V_p and V_s wave velocities at different grid spacing to access the resolution of our data set. We found that the present data set is able to resolve the 3-D velocity (V_p and V_s) structures with a size of 30 km horizontal and 5 km vertical near the Bhuj mainshock.

[13] In order to ensure the resolvability of the obtained velocity anomalies (V_p and V_s) in our tomographic inversion, we also conducted synthetic tests. The synthetic models for both V_p and V_s at 25 km depth are shown in Figures 5a and 5b. The inverted images (Figures 5c and 5d) of both V_p and V_s , clearly indicate that the anomalies at the mainshock hypocenter are well reconstructed.

4. Concluding Remarks

[14] We determined detailed 3-D V_p , V_s , and σ structures in the source area of the 2001 Bhuj earthquake using a large

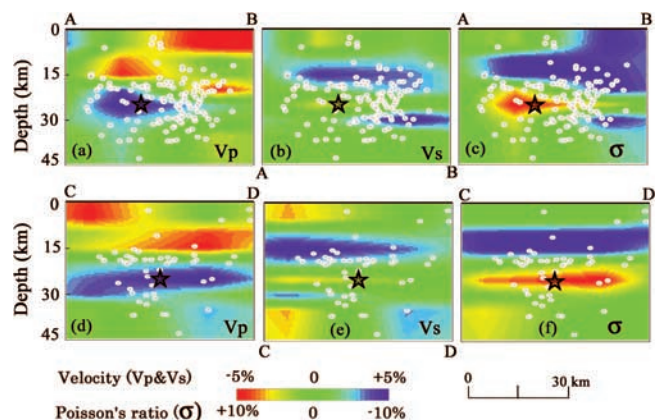


Figure 4. (a–c) Vertical cross sections along the line A–B for V_p , V_s and σ , respectively. (d–f) represent a cross section along the line C–D for V_p , V_s and σ , respectively. Small white circles show Bhuj aftershocks within 9-km width along the lines A–B and C–D. The star, Bhuj mainshock hypocenter; its focal depth is 25.0 km. The perturbation (in %) scales are shown at the bottom.

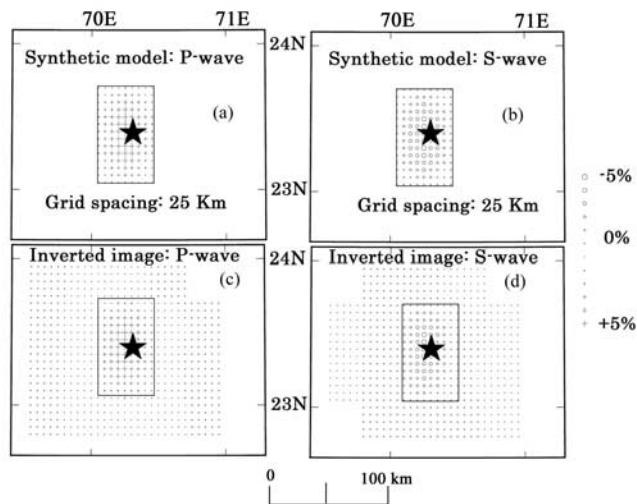


Figure 5. (a–b) Synthetic models for V_p and V_s at a grid spacing of 25 km, respectively. (c–d) Inverted images for V_p and V_s , respectively. Star denotes Bhuj mainshock hypocenter. The black boxes denote the zones of synthetic anomalies (a–b) and reconstructed anomalies (c–d) after inversion. The perturbation scale (in %) is shown on the right side.

number of high-quality P and S wave arrivals. The source zone of Bhuj hypocenter is characterized anomalously by high- V_p , low- V_s and high- σ , indicating the presence of fluid-filled, fractured rock matrix in the source zone, which might have affected the long-term structural and compositional evolution of the fault zone, the fault zone strength, and the local stress regime of the source area on enhancing the stress concentration in the seismogenic layer. Consequently, it may lead to a mechanical failure of asperities and barriers and thus might have contributed to the initiation of the 2001 Bhuj earthquake. Our present results are similar to those that were found for the 1995 Kobe earthquake [Zhao *et al.*, 1996]. In future studies the use of not only seismic but also other geophysical methods (e.g. geoelectric prospecting, magnetotelluric sounding and gravity) and hydrological observations can yield a better understanding of the fault zone, which contains the over pressurized fluids.

[15] **Acknowledgments.** We would like to thank the research group of Geological Survey of India, for collecting high quality aftershock data, which we have used in this study. The authors thank the research group of Geodynamics Research Center, Ehime University, Japan for all along assistance at the data processing stage. We benefited from the critical reviews and thoughtful comments from two anonymous referees, which improved the manuscript. This work was partially supported by a grant

(Kiban-B No. 11440134) from the Japan Society for the Promotion of Science to D. Zhao.

References

- Biswas, S. K., Regional tectonic framework, structure and evolution of the western marginal basins of India, *Tectonophysics*, 135, 307–327, 1987.
- Eberhart-Phillips, D., and A. J. Michael, Three-dimensional velocity structure, seismicity, and fault structure in the Parkfield region, central California, *J. Geophys. Res.*, 98, 15,737–15,758, 1993.
- GSI, Seismotectonic Atlas of India and its Environs, *Geol. Surv. India Sp. Pub.*, 39, 2000.
- Gupta, H. K., S. V. S. Sarma, T. Harinarayana, and G. Virupakshi, Fluids below the hypocentral region of Latur earthquake, India: Geophysical indicators, *Geophys. Res. Lett.*, 23, 1569–1572, 1996.
- Johnston, A. C., and L. R. Kanter, Earthquakes in stable continental crust, *Am. J. Science*, 262, 68–75, 1990.
- Kayal, J. R., and S. Mukhopadhyay, Seismic tomography structure of the 1993 Killari earthquake source area, submitted, *Bull. Seism. Soc. Am*, 2002.
- Kayal, J. R., R. De, S. Ram, B. V. Srirama, and S. G. Gaonkar, Aftershocks of the January 26, 2001 Bhuj earthquake and its seismotectonic implications, submitted, *J. Geol. Soc. India*, 59, 395–417, 2002.
- Krishna, J., Seismic zoning maps of India, *Curr. Sci*, 62, 17–23, 1992.
- Lees, J. M., Tomographic P-wave velocity images of the Loma Prieta earthquake asperity, *Geophys. Res. Lett.*, 17, 1433–1436, 1990.
- O'Connell, R. J., and B. Budiansky, Seismic velocities in dry and saturated cracked solids, *J. Geophys. Res.*, 79, 5412–5426, 1974.
- Oldham, R. D., The Cutch earthquake of 16th June, 1819 with a revision of the great earthquake of 12th June, 1997, *Mem. Geol. Surv. India*, 46, 1–77, 1926.
- Shanker, R., and P. Pande, Geoseismological studies of Kutch (Bhuj) earthquake of 26 January, 2001, *J. Geol. Soc. India*, 58, 203–208, 2001.
- Srinagesh, D., S. Singh, K. Srinath Reddy, K. S. Prakasam, and S. S. Rai, Evidence for high velocity in Koyna Seismic zone from P-wave teleseismic imaging, *Geophys. Res. Lett.*, 27, 2737–2740, 2000.
- Thurber, C., S. Roecker, W. Ellsworth, Y. Chen, W. Lutter, and R. Sessions, Two-dimensional seismic image of the San Andreas fault in the Northern Gabilan Range, central California: Evidence for fluids in the fault zone, *Geophys. Res. Lett.*, 24, 1591–1594, 1997.
- Zhao, D., A. Hasegawa, and S. Horiuchi, Tomographic imaging of P and S wave velocity structure beneath northeastern Japan, *J. Geophys. Res.*, 97, 19,909–19,928, 1992.
- Zhao, D., and H. Kanamori, The 1992 Lander earthquake sequence: Earthquake occurrence and structural heterogeneities, *Geophys. Res. Lett.*, 20, 1083–1086, 1993.
- Zhao, D., and H. Kanamori, The 1994 North ridge earthquake: 3-D crustal structure in the rupture zone and its relation to the aftershock locations and mechanisms, *Geophys. Res. Lett.*, 22, 736–766, 1995.
- Zhao, D., H. Kanamori, and H. Negishi, Tomography of the source area of the 1995 Kobe earthquake: evidence for fluids at the hypocenter?, *Science*, 274, 1891–1894, 1996.
- Zhao, D., and H. Negishi, The 1995 Kobe earthquake: seismic image of the source zone and its implications for the rupture nucleation, *J. Geophys. Res.*, 103, 9967–9986, 1998.

J. R. Kayal, R. De, and O. P. Singh, Geological Survey of India, 27 J.L. Nehru Road, Calcutta 700 016, India.

D. Zhao and O. P. Mishra, Geodynamics Research Center, Ehime University, Matsuyama 790-8577, Japan.